Int. J. Adv. Appl. Math. and Mech. 2(1) (2014) 107 - 119
ISSN: 2347-2529
Available online at www.ijaamm.com

IJAAMM

International Journal of Advances in **Applied Mathematics and Mechanics**

Soret-Dufour and Radiation effect on unsteady MHD flow over an inclined porous plate embedded in porous medium with viscous dissipation

Research Article

N. Pandya[1], A. K. Shukla[2,] *

[1]*Department of mathematics and astronomy, University of Lucknow, Lucknow-226007, India*

[2]*Department of mathematics and astronomy, University of Lucknow, Lucknow-226007, India*

Received 08 June 2014; accepted (in revised version) 23 August 2014

Abstract: We study Soret-Dufour and radiation effects on unsteady viscous incompressible MHD flow along semi infinite inclined permeable moving plate with variable temperature and mass diffusion embedded in a porous medium numerically, by taking into account the effect of viscous dissipation. The dimensionless governing equations of flow field are solved numerically by Crank-Nicolson finite difference method for different values of governing flow parameters. The velocity temperature, concentration, skin-friction, Nusselt number, Sherwood number are shown through graphs and tables.

MSC: 76W05 • 76R50 • 78A40 • 76M20

Keywords: MHD • Soret effect • Dufour effect • thermal radiation • porous medium • Heat and mass transfer • Crank-Nicolson method

1. Introduction

Soret-Dufour and radiation effect on MHD flows arise in many areas of engineering and applied physics. The study of such flow has application in MHD generators, chemical engineering, nuclear reactors, geothermal energy, reservoir engineering and astrophysical studies. In nature, the assumption of the pure fluid is rather impossible. The presence of foreign mass in the fluid plays an important role in flow of fluid.

Thermal diffusion or Soret effect is one of the mechanisms in the transport phenomena in which molecules are transported in a multi-component mixture driven by temperature gradient. The inverse phenomena of thermal diffusion, if multi component mixture were initially at the same temperature, are allowed to diffuse into each other, there arises a difference of temperature in the system. Sparrow and Cess[1] analyzed the effect of magnetic field on free convection heat transfer Alam et al.[2] investigated Dufour effect and Soret effect on MHD free convective heat and mass transfer flow past a vertical flat plate embedded in porous medium. Dursunkaya et al.[3] studied Diffusion-thermo and thermal diffusion effect in transient and steady natural convection from vertical surface, Postelnicu[4] analyzed the influence of a magnetic field on heat and mass transfer by natural convection from vertical surface in porous media considering Soret and Dufour effects. Raptis et al.[5] discussed radiation and free convection flow past a moving plate.

Rajesh and Vijaya kumar verma[6] analyzed radiation and mass transfer effects on MHD free convection flow past an exponentially accelerated vertical plate with variable temperature. Satyanarayana[7] discussed the viscous dissipation and thermal radiation effects on an unsteady MHD convection flow past a semi infinite vertical permeable

* Corresponding author.
E-mail address: ashishshukla1987@gmail.com

moving porous plate. Shivaiah[8] analyzed chemical reaction effects on an unsteady MHD free convective flow past and infinite vertical porous plate with constant suction and heat source. Alabraba et al.[9] investigated the interaction of mixed convection with thermal radiation in laminar boundary flow taking into account the binary chemical reaction and Soret-Dufour effects. Karim et al.[10] investigated Dufour and Soret effect on steady MHD flow in presence of heat generation and magnetic field past an inclined stretching sheet. Recently Bhavana et al.[11] analyzed the Soret effect on free convective unsteady MHD flow over a vertical plate with heat source.
The objective of this work is to analyze the effects of Soret-Dufour and radiation effects on unsteady MHD flow over a inclined porous plate embedded in porous medium with viscous dissipation. The dimensionless governing equations of flow field are solved numerically using Crank-Nicolson implicit finite difference method. The effect of different flow parameters on velocity, temperature, concentration, skin friction, Nusselt number and Sherwood number are discussed and shown through graphs and tables.

2. Mathematical analysis

An unsteady flow of a viscous incompressible electrically conducting fluid past an impulsively started infinite inclined porous plate with variable temperature and variable mass diffusion with radiation and viscous dissipation are studied. The plate is inclined at angle α to vertical, is embedded in porous medium. x'-axis is taken along the plate and y'-axis is taken normal to it. It is also considered that the radiation heat flux in x'-direction is negligible in comparison to y'-direction. Initially the plate and fluid are at the same temperature T'_∞ and concentration level C'_∞. At time $t' > 0$, the plate is moving impulsive motion along x'-direction against gravitational field with constant velocity u_0 , the plate temperature and concentration raised linearly with time t' . A transverse magnetic field of uniform strength B_0 is assumed normal to the direction of flow. The transversely applied magnetic field and magnetic Reynolds number are very small and hence induced magnetic field is negligible, Cowling[12].
Due to infinite length in x' -direction, the flow variables are functions of y' and t' only. Under the usual Boussinesq approximation, governing equations for this unsteady problem are given by
Continuity equation:

$$\frac{\partial v'}{\partial y'} = 0 \Rightarrow v' = -v_0 (constant) \tag{1}$$

Momentum equation:

$$\frac{\partial u'}{\partial t'} + v' \frac{\partial u'}{\partial y'} = \nu \frac{\partial^2 u'}{\partial y'^2} + g\beta(T' - T'_\infty) cos(\alpha) + g\beta^*(C' - C'_\infty) cos(\alpha) - \frac{\sigma B_0^2 u'}{\rho} - \frac{\nu u'}{K'} \tag{2}$$

Energy equation:

$$\rho C_p \left(\frac{\partial T'}{\partial t'} + v' \frac{\partial T'}{\partial y'} \right) = k \frac{\partial^2 T'}{\partial y'^2} - \frac{\partial q_r}{\partial y'} + \frac{\rho D_m K_T}{c_s} \frac{\partial^2 C'}{\partial y'^2} + \mu \left(\frac{\partial u'}{\partial y'} \right)^2 \tag{3}$$

Equation of continuity for mass transfer:

$$\frac{\partial C'}{\partial t'} + v' \frac{\partial C'}{\partial y'} = D \frac{\partial^2 C'}{\partial y'^2} + \frac{D_m K_T}{T_m} \frac{\partial^2 T'}{\partial y'^2} \tag{4}$$

where u' and v' is the velocity component along x'-direction and y'- direction respectively. g is the acceleration due to gravity, β is the volumetric coefficient of thermal expansion, β^* is the coefficient of volume expansion for mass transfer, ν is the kinematic viscosity, μ is viscosity, ρ is the fluid density, B_0 is magnetic induction, K' is the permeability of porous medium, σ is the electrical conductivity of the fluid, T' is the dimensional temperature, T'_∞ is temperature of free stream, C'_∞ is concentration of free stream, D_m is the chemical molecular diffusivity, k is the thermal conductivity of the fluid , c_p is specific heat at constant pressure, K_T is thermal diffusion ratio, C' is the dimensional concentration, q_r is radiative heat flux in y'-direction, T_m is mean fluid temperature.
Initial and boundary conditions are given as:

$$\begin{aligned} & t' \le 0 \quad u' = 0 \quad T' = T'_\infty \quad C' = C'_\infty \quad \forall y' \\ t' > 0 \quad & u' = u_0 \quad v' = -v_0 \quad T' = T' + (T'_w - T'_\infty) e^{At'}, \\ & C' = C' + (C'_w - C'_\infty) e^{At'} \quad at\ y' = 0 \\ & u' = 0 \quad T' \to \infty \quad C' \to \infty \quad y' \to \infty \end{aligned} \tag{5}$$

where, $A = \frac{v_0^2}{\nu}$, T'_w and C'_w are tmeperature and concentration of plate respectively.
The radiative heat flux term by using the Roseland approximation is given by

$$q_r = -\frac{4\sigma}{3k_l} \frac{\partial T'^4}{\partial y'} \tag{6}$$

where k_l and σ are mean absorption coefficient and Stefan Boltzmann constant respectively. It is assumed that the temperature difference within the flow are sufficiently small such that T'^4 may be expressed as a linear function of the temperature. This is accomplished by expanding in a Taylor series about T'_∞ and neglecting the higher order terms, thus

$$T'^4 \cong 4T'^3_\infty T' - 3T'^4_\infty \tag{7}$$

then using Eqs. (6) and (7), Eq. (3) is reduced

$$\rho C_p\left(\frac{\partial T'}{\partial t'} + v'\frac{\partial T'}{\partial y'}\right) = k\frac{\partial^2 T'}{\partial y'^2} + \frac{16\sigma T'^3_\infty}{3k_l}\frac{\partial^2 T'}{\partial y'^2} + \frac{\rho D_m K_T}{c_s}\frac{\partial^2 C'}{\partial y'^2} + \mu\left(\frac{\partial u'}{\partial y'}\right)^2 \tag{8}$$

In order to acquire non-dimensional partial differential equations, introducing following dimensionless quantities:

$$\begin{gathered} u = \frac{u'}{u_0},\ t = \frac{t' v_0^2}{\nu},\ \theta = \frac{T' - T'_\infty}{T'_w - T'_\infty},\ C = \frac{C' - C'_\infty}{C'_w - C'_\infty},\ Gm = \frac{\nu g\beta^*(C'_w - C'_\infty)}{u_0 v_0^2}, \\ Gr = \frac{\nu g\beta(T'_w - T'_\infty)}{u_0 v_0^2},\ Du = \frac{D_m K_T(C'_w - C'_\infty)}{c_s c_p \nu(T'_w - T'_\infty)},\ Sr = \frac{D_m K_T(T'_w - T'_\infty)}{T_m \nu(C'_w - C'_\infty)}, \\ K = \frac{v_0^2 K'}{\nu^2},\ Pr = \frac{\mu c_p}{k},\ M = \frac{\sigma B_0^2 \nu}{\rho v_0^2},\ R = \frac{4\sigma T'^3_\infty}{k_l k}, \\ Sc = \frac{\nu}{D_m},\ Ec = \frac{u_0^2}{c_p(T'_w - T'_\infty)},\ y = \frac{y' v_0}{\nu} \end{gathered} \tag{9}$$

By merit of Eq. (9), we obtain non-dimensional form of Eqs. (2), (3) and (8) respectively:

$$\frac{\partial u}{\partial t} - \frac{\partial u}{\partial y} = \frac{\partial^2 u}{\partial y^2} + Gr\cos(\alpha) + Gm\cos(\alpha) - \left(M + \frac{1}{K}\right)u \tag{10}$$

$$\frac{\partial \theta}{\partial t} - \frac{\partial \theta}{\partial y} = \frac{1}{Pr}\left(1 + \frac{4R}{3}\right)\frac{\partial^2 \theta}{\partial y^2} + Du\frac{\partial^2 C}{\partial y^2} + Ec\left(\frac{\partial u}{\partial y}\right)^2 \tag{11}$$

$$\frac{\partial C}{\partial t} - \frac{\partial C}{\partial y} = \frac{1}{Sc}\frac{\partial^2 C}{\partial y^2} + Sr\frac{\partial^2 \theta}{\partial y^2} \tag{12}$$

with following initial and boundary conditions in non-dimensional form are:

$$\begin{aligned} &t \le 0 \quad u = 0 \quad \theta = 0 \quad C = 0 \quad \forall y \\ &t > 0 \quad u = 1 \quad \theta = e^t \quad C = e^t \quad at\ y = 0 \\ &\qquad u = 0 \quad u \to 0 \quad C \to 0 \quad y \to 0 \end{aligned} \tag{13}$$

Now it is important to calculate the physical quantities of primary interest, which are the local shear stress, local surface heat flux and Sherwood number.
dimensionless local wall shear stress or skin-friction is obtained as,

$$\tau = \left(\frac{\partial u}{\partial y}\right)_{y=0} \tag{14}$$

dimensionless local surface heat flux or Nusselt number is obtained as

$$Nu = -\left(\frac{\partial \theta}{\partial y}\right)_{y=0} \tag{15}$$

dimensionless the local Sherwood number is obtained as

$$Sh = -\left(\frac{\partial C}{\partial y}\right)_{y=0} \tag{16}$$

3. Method of solution

Eqs. (10)-(12) are coupled non-linear partial differential equations are solved using boundary and initial conditions (13). All the same, exact or approximate solutions are not possible. Therefore we solve these equations by Crank-Nicolson implicit finite difference method for numerical solution. The equivalent finite difference scheme of Eqs. (10)-(12) are as follows:

$$\frac{u_{i,j+1}-u_{i,j}}{\Delta t}-\frac{u_{i+1,j}-u_{i,j}}{\Delta y}=\left(\frac{u_{i-1,j}-2u_{i,j}+u_{i-1,j}-2u_{i,j+1}+u_{i+1,j+1}}{2(\Delta y)^2}\right)$$
$$+Gr\,cos(\alpha)\left(\frac{\theta_{i,j+1}-\theta_{i,j}}{2}\right)+Gm\,cos(\alpha)\left(\frac{Ci,j+1-Ci,j}{2}\right) \tag{17}$$
$$-\left(M+\frac{1}{K}\right)\left(\frac{u_{i,j+1}+u_{i,j}}{2}\right)$$

$$\frac{\theta_{i,j+1}-\theta_{i,j}}{\Delta t}-\frac{\theta_{i+1,j}-\theta_{i,j}}{\Delta y}=\frac{1}{Pr}\left(1+\frac{4R}{3}\right)\left(\frac{\theta_{i-1,j}-2\theta_{i,j}+\theta_{i-1,j}-2\theta_{i,j+1}+\theta_{i+1,j+1}}{2(\Delta y)^2}\right)$$
$$+Du\left(\frac{C_{i-1,j}-2u_{i,j}+C_{i-1,j}-2C_{i,j+1}+C_{i+1,j+1}}{2(\Delta y)^2}\right) \tag{18}$$
$$+Ec\left(\frac{u_{i+1,j}-u_{i,j}}{\Delta y}\right)^2$$

$$\frac{C_{i,j+1}-C_{i,j}}{\Delta t}-\frac{C_{i+1,j}-C_{i,j}}{\Delta y}=\frac{1}{Sc}\left(\frac{C_{i-1,j}-2u_{i,j}+C_{i-1,j}-2C_{i,j+1}+C_{i+1,j+1}}{2(\Delta y)^2}\right)$$
$$+Sr\left(\frac{\theta_{i-1,j}-2\theta_{i,j}+\theta_{i-1,j}-2\theta_{i,j+1}+\theta_{i+1,j+1}}{2(\Delta y)^2}\right) \tag{19}$$

corresponding boundary and initial conditions are

$$\begin{aligned} u_{i,0}=0 \quad \theta_{i,0}=0 \quad C_{i,0}=0 \quad \forall\, i \\ u_{0,j}=1 \quad \theta_{0,j}=e^{j\Delta t} \quad C_{0,j}=e^{j\Delta t} \\ u_{X,j}=0 \quad \theta_{X,j}\to 0 \quad C_{X,j}\to 0 \end{aligned} \tag{20}$$

Here index i refers to y and j refers to time t, $\Delta t=t_{j+1}-t_j$ and $\Delta y=y_{i+1}-y_i$. Knowing the values of u, θ and C at time t , we can compute the values at time $t+\Delta t$ as follows: we substitute $i=1,2,...,N-1$, where N correspond to ∞ , in Eqs. (17)-(19) which make up tridiagonal system of equations, can be figured out by Thomas algorithm as discussed in Carnahan et al.[13]. Subsequently θ and C are known for all values of y at time $t+\Delta t$. Replace these values of and in equation (17) and solved by same procedure with initial and boundary condition, we obtain solution for u till desired time t .

The implicit Crank-Nicolson finite difference method is a second order method $\left(o\left(\Delta t^2\right)\right)$ in time and has no restriction on space and time steps, that is, the method is unconditionally stable. The computation is executed for $\Delta y=0.1$, $\Delta t=0.001$ and procedure is repeated till $y=4$.

4. Result and discussion

Soret-Dufour and radiation effects on unsteady MHD flow past an inclined porous plate embedded in porous medium with variable temperature and variable mass diffusion in presence of viscous dissipation. The governing equations are solved by using Crank-Nicolson implicit finite difference method and solutions are obtained for velocity field, temperature field, concentration field, skin-friction, Nusselt number and Sherwood number. The consequences of the relevant parameters on the flow field are broke down and discussed with the help of graphs of velocity profiles, temperature profiles, concentration profiles and tables of skin-friction coefficient, Nusselt number, Sherwood number.

Figs. 7 and 15 depict the variation of velocity field u against Prandtl number Pr and magnetic parameter M. It is observed when Pr and M increase velocity decreases. It is analyzed in Figs. 21 and 4 when inclination angle α and Schmidt number Sc raise, velocity decreases. Increasing radiation parameter R and permeability K, it is observed that velocity increases in Figs. 17 and 20 respectively. It is dissected in Figs. 14 and 13 when Grashof number Gr and solutal Grashof number Gm increase, velocity increases. Figs. 1 and 10 describe when Soret number Sr and Dufour number Du increase, velocity increases and decreases respectively. Increasing Eckert number Ec and time t in Figs. 25 and 22, velocity increases also.

Figs. 8 and 5 depict that increasing Prandtl number Pr, temperature decreases and increasing Schmidt number Sc, first temperature increases later on decreases. Similarly in Figs. 2, increasing Soret number Sr, temperature increases in beginning afterward decreases. It is analyzed in Figs. 11 that temperature decreases as Dufour number increases. Figs. 26 , 18 and 23 show when Eckert number Ec, radiation parameter R and time t increase, temperature increases.
Figs. 9 displays that increasing Prandtl number Pr, in starting concentration increases afterward decreases. It is observed in Figs. 3 and 6 when Soret number Sr and Schmidt number Sc increases, concentration increases and decreases respectively. Increasing Dufour number Du, in beginning concentration increases then decreases in Figs. 12. It is analyzed in Figs. 19 and 16, first concentration diminishes later on raises as radiation parameter R and Eckert number Ec increase. Figs. 24 demonstrates that increasing time t, concentration increases.

Table 1 displays that enhancing Dufour number Du, Eckert number Ec, Solutal Grashof number Gm, Grashof number Gr, permeability parameter K, Prandtl number Pr, radiation parameter R, Soret number Sr and time t, skin-friction coefficient increases. And increasing inclination angle α , magnetic parameter M and Schmidt number Sc, skin-friction coefficient decreases.

Table 2 shows that raising Dufour number Du, Prandtl number Pr, Soret number Sr, Nusselt number Nu increases. Increasing inclination angle α , Eckert number Ec, radiation parameter R, Schmidt number Sc, time t, Nusselt number Nu decreases.

Table 3 exhibits that increasing inclination angle α , radiation parameter R, Schmidt number Sc, Sherwood number Sh increases. Enhancing Dufour number Du, Prandtl number Pr, Soret number Sr, time t, Sherwood number Sh decreases.

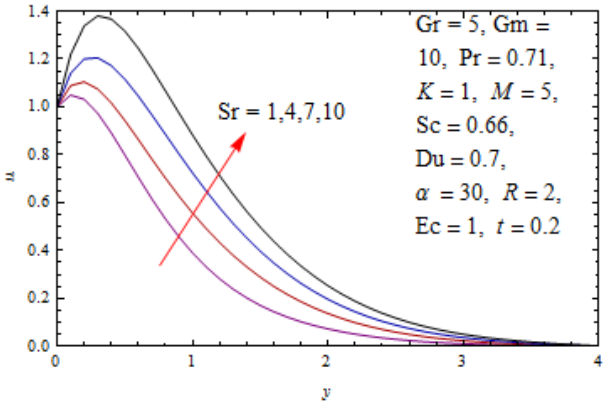

Fig. 1. Velocity Profile for Different Values of Sr

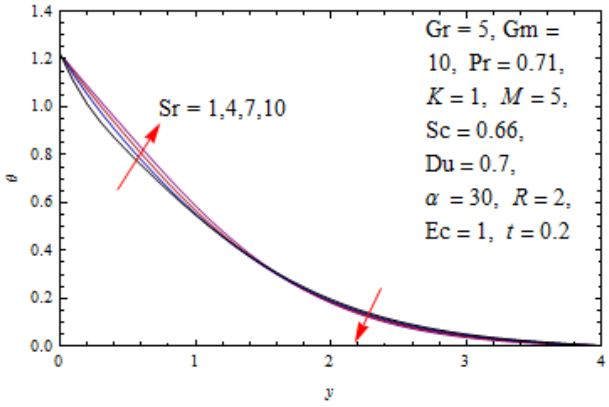

Fig. 2. Temperature Profile for Different Values of Sr

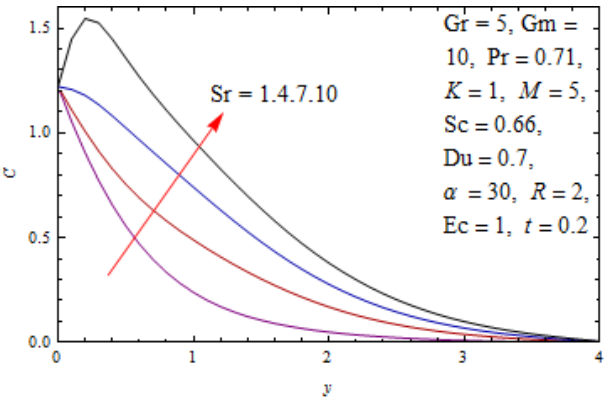

Fig. 3. Concentration Profile for Different Values of Sr

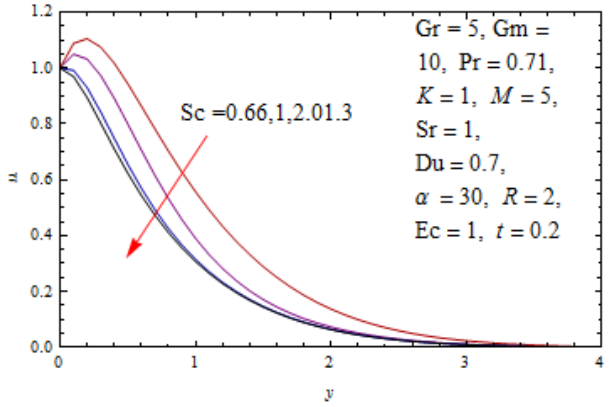

Fig. 4. Velocity Profile for Different Values of Sc

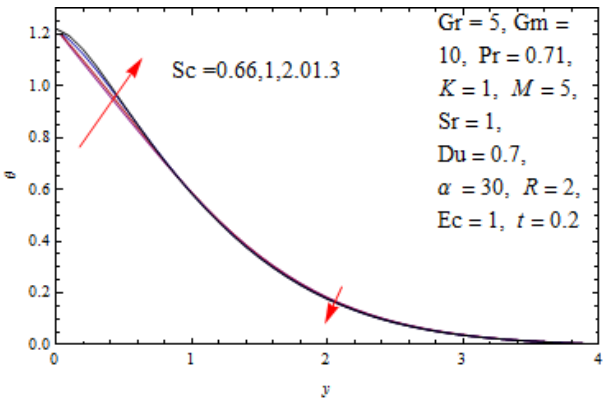

Fig. 5. Temperature Profile for Different Values of Sc

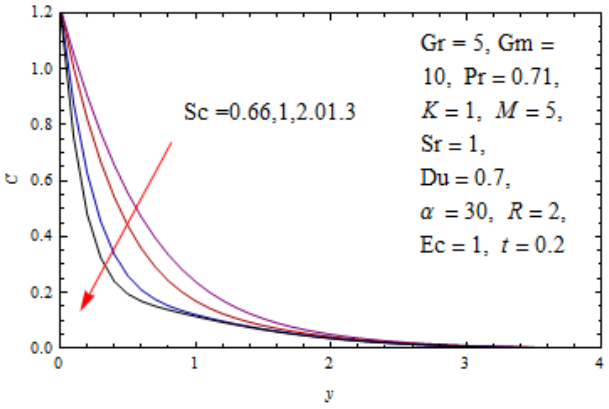

Fig. 6. Concentration Profile for Different Values of Sc

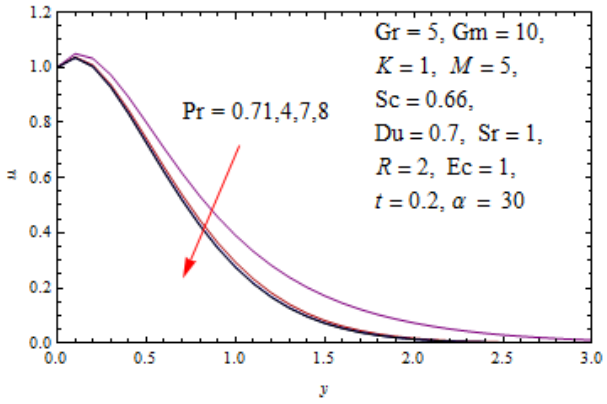

Fig. 7. Velocity Profile for Different Values of Pr

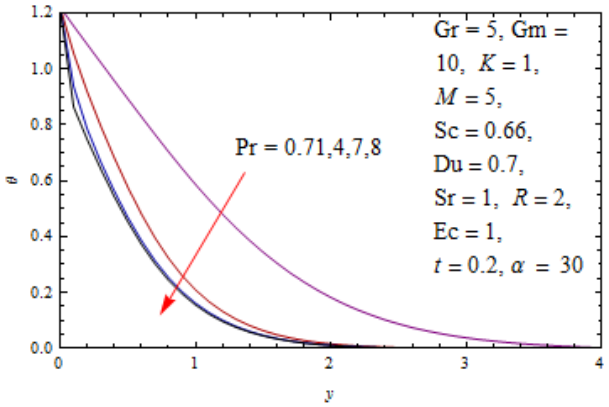

Fig. 8. Temperature Profile for Different Values of Pr

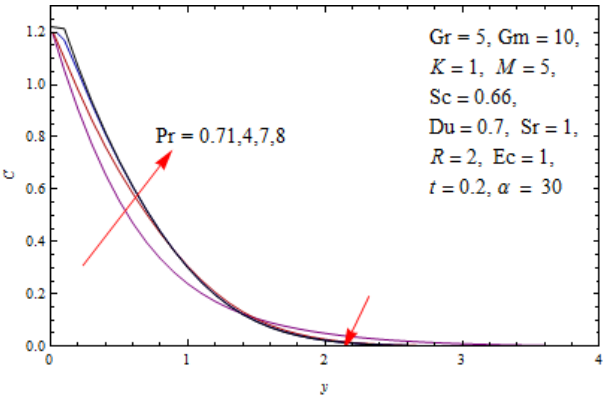

Fig. 9. Concentration Profile for Different Values of Pr

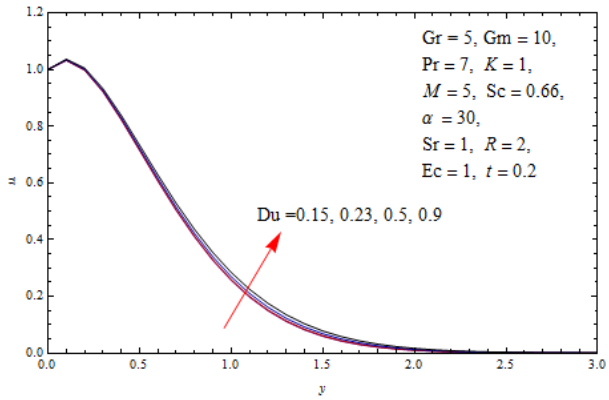

Fig. 10. Velocity Profile for Different Values of Du

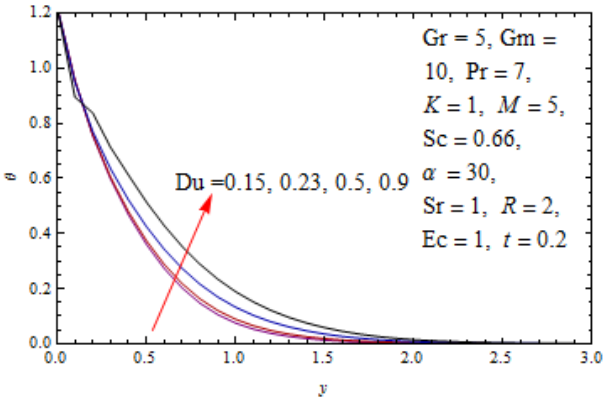

Fig. 11. Temperature Profile for Different Values of Du

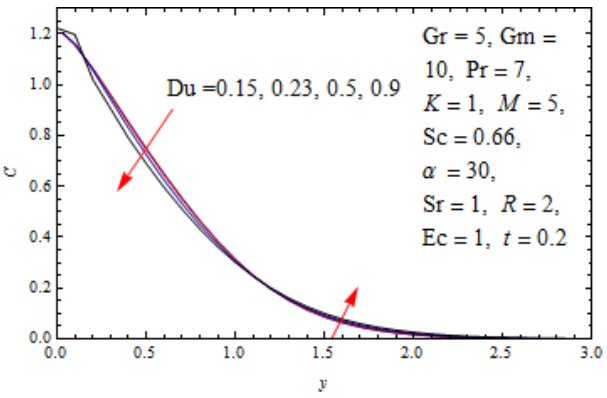

Fig. 12. Concentration Profile for Different Values of Du

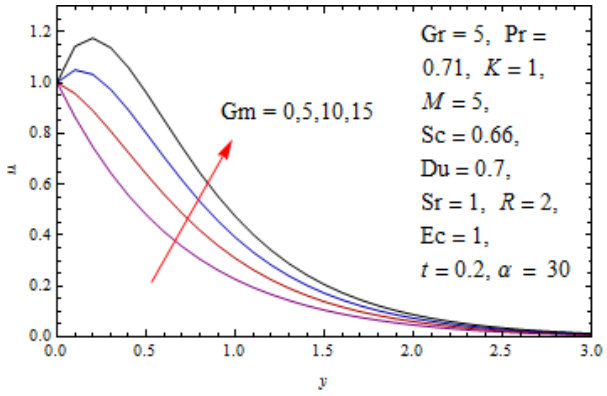

Fig. 13. Velocity Profile for Different Values of Gm

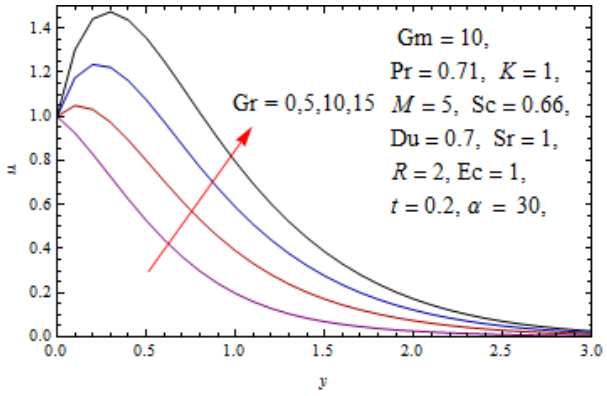

Fig. 14. Velocity Profile for Different Values of Gr

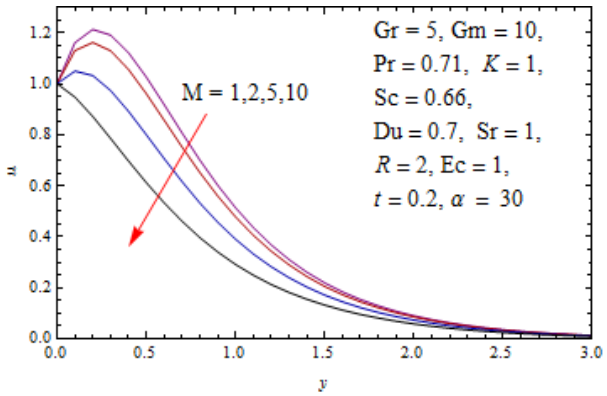

Fig. 15. Velocity Profile for Different Values of M

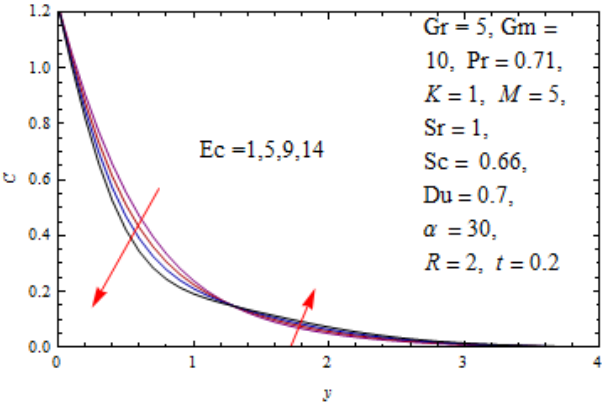

Fig. 16. Concentration Profile for Different Values of Ec

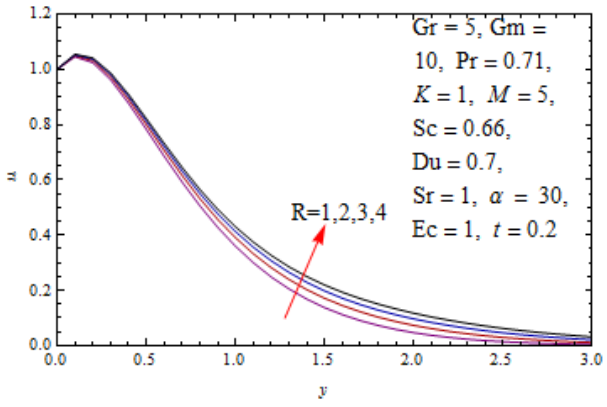

Fig. 17. Velocity Profile for Different Values of R

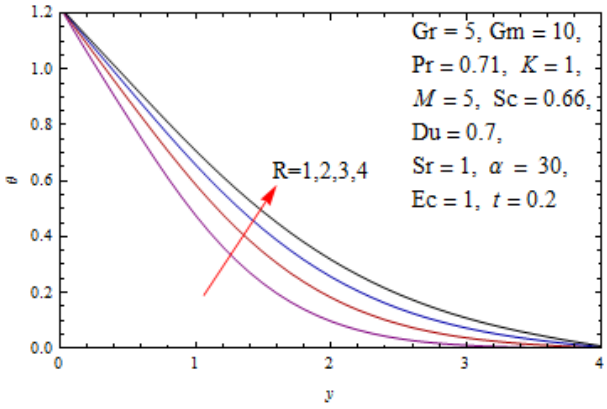

Fig. 18. Temperature Profile for Different Values of R

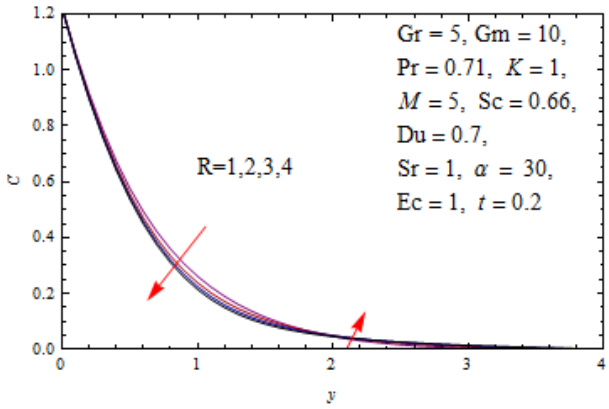

Fig. 19. Concentration Profile for Different Values of R

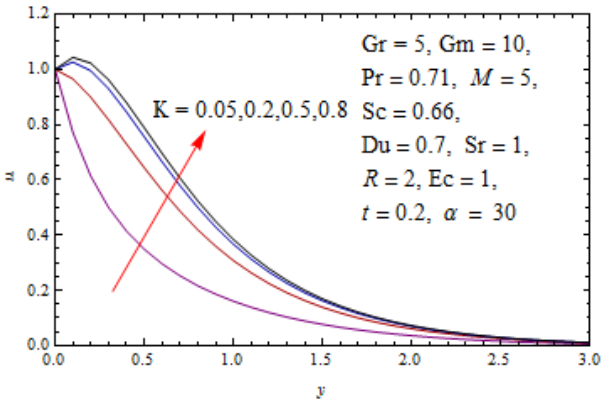

Fig. 20. Velocity Profile for Different Values of K

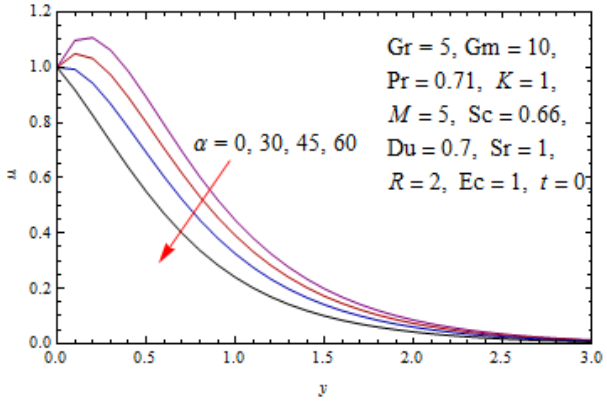

Fig. 21. Velocity Profile for Different Values of λ

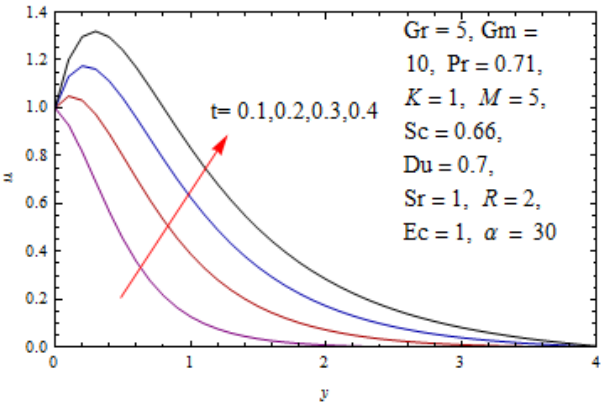

Fig. 22. Velocity Profile for Different Values of t

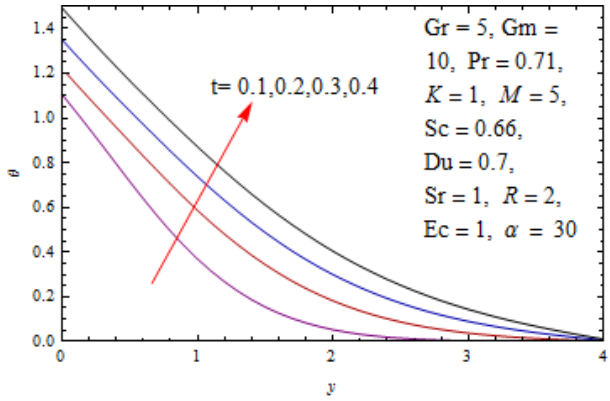

Fig. 23. Temperature Profile for Different Values of t

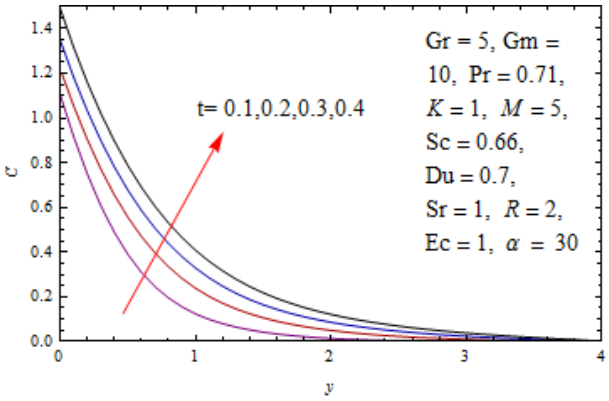

Fig. 24. Concentration Profile for Different Values of t

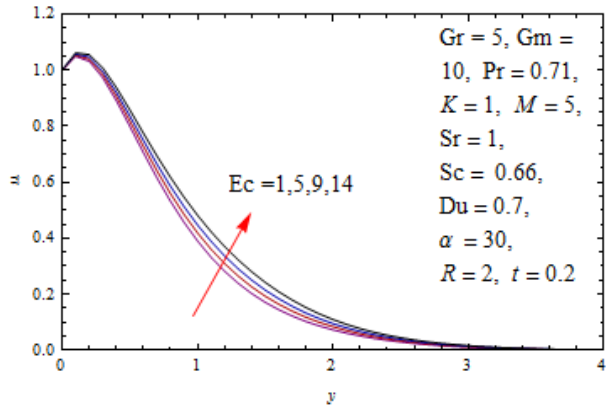

Fig. 25. Velocity Profile for Different Values of Ec

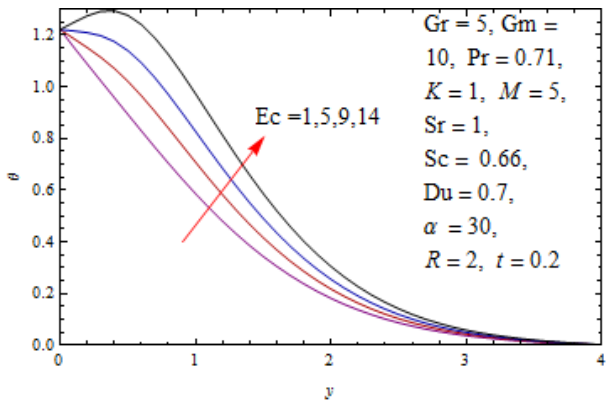

Fig. 26. Temperature Profile for Different Values of Ec

Table 1. Skin friction coefficient τ for different values of parameters

t	R	Pr	M	K	Sc	Sr	α	Du	Gm	Gr	Ec	τ
0.2	1	0.71	5	1	0.66	1	30	0.7	10	5	1	0.458197
0.2	3	0.71	5	1	0.66	1	30	0.7	10	5	1	0.523628
0.2	4	0.71	5	1	0.66	1	30	0.7	10	5	1	0.544682
0.2	2	4	5	1	0.66	1	30	0.7	10	5	1	0.372707
0.2	2	7	5	1	0.66	1	30	0.7	10	5	1	0.351861
0.2	2	8	5	1	0.66	1	30	0.7	10	5	1	0.349694
0.2	2	0.71	1	1	0.66	1	30	0.7	10	5	1	1.60966
0.2	2	0.71	2	1	0.66	1	30	0.7	10	5	1	1.29914
0.2	2	0.71	10	1	0.66	1	30	0.7	10	5	1	−0.526618
0.2	2	0.71	5	0.05	0.66	1	30	0.7	10	5	1	−2.2865
0.2	2	0.71	5	0.2	0.66	1	30	0.7	10	5	1	−0.346674
0.2	2	0.71	5	0.5	0.66	1	30	0.7	10	5	1	0.264523
0.2	2	0.71	5	0.8	0.66	1	30	0.7	10	5	1	0.436886
0.2	2	0.71	5	1	1	1	30	0.7	10	5	1	0.287898
0.2	2	0.71	5	1	2.01	1	30	0.7	10	5	1	−0.0847133
0.2	2	0.71	5	1	3	1	30	0.7	10	5	1	−0.307713
0.2	2	0.71	5	1	0.66	4	30	0.7	10	5	1	0.883421
0.2	2	0.71	5	1	0.66	7	30	0.7	10	5	1	1.40196
0.2	2	0.71	5	1	0.66	10	30	0.7	10	5	1	2.18625
0.2	2	0.71	5	1	0.66	1	0	0.7	10	5	1	0.976127
0.2	2	0.71	5	1	0.66	1	45	0.7	10	5	1	−0.0721526
0.2	2	0.71	5	1	0.66	1	60	0.7	10	5	1	−0.812158
0.2	2	7	5	1	0.66	1	30	0.15	10	5	1	0.322698
0.2	2	7	5	1	0.66	1	30	0.23	10	5	1	0.326735
0.2	2	7	5	1	0.66	1	30	0.5	10	5	1	0.340833
0.2	2	7	5	1	0.66	1	30	0.9	10	5	1	0.363698
0.2	2	0.71	5	1	0.66	1	30	0.7	0	5	1	−1.3527
0.2	2	0.71	5	1	0.66	1	30	0.7	5	5	1	−0.428495
0.2	2	0.71	5	1	0.66	1	30	0.7	15	5	1	1.42055
0.2	2	0.71	5	1	0.66	1	30	0.7	10	5	1	−0.753363
0.2	2	0.71	5	1	0.66	1	30	0.7	10	5	1	1.75057
0.2	2	0.71	5	1	0.66	1	30	0.7	10	5	1	3.01956
0.2	2	0.71	5	1	0.66	1	30	0.7	10	5	5	0.535
0.2	2	0.71	5	1	0.66	1	30	0.7	10	5	9	0.571954
0.2	2	0.71	5	1	0.66	1	30	0.7	10	5	14	0.615956
0.1	2	0.71	5	1	0.66	1	30	0.7	10	5	1	−0.710751
0.3	2	0.71	5	1	0.66	1	30	0.7	10	5	1	1.31261
0.4	2	0.71	5	1	0.66	1	30	0.7	10	5	1	2.01698

Table 2. Nusselt number for different values of parameters

t	R	Pr	M	K	Sc	Sr	α	Du	Gm	Gr	Ec	Nu
0.2	1	0.71	5	1	0.66	1	30	0.7	10	5	1	0.823538
0.2	3	0.71	5	1	0.66	1	30	0.7	10	5	1	0.585463
0.2	4	0.71	5	1	0.66	1	30	0.7	10	5	1	0.527495
0.2	2	4	5	1	0.66	1	30	0.7	10	5	1	1.6441
0.2	2	7	5	1	0.66	1	30	0.7	10	5	1	2.83998
0.2	2	8	5	1	0.66	1	30	0.7	10	5	1	3.57114
0.2	2	0.71	5	1	1	1	30	0.7	10	5	1	0.60778
0.2	2	0.71	5	1	2.01	1	30	0.7	10	5	1	0.440804
0.2	2	0.71	5	1	3	1	30	0.7	10	5	1	0.286246
0.2	2	0.71	5	1	0.66	4	30	0.7	10	5	1	0.750167
0.2	2	0.71	5	1	0.66	7	30	0.7	10	5	1	0.866699
0.2	2	0.71	5	1	0.66	10	30	0.7	10	5	1	1.14459
0.2	2	7	5	1	0.66	1	30	0.15	10	5	1	2.65431
0.2	2	7	5	1	0.66	1	30	0.23	10	5	1	2.66072
0.2	2	7	5	1	0.66	1	30	0.5	10	5	1	2.71652
0.2	2	7	5	1	0.66	1	30	0.9	10	5	1	3.626008
0.2	2	0.71	5	1	0.66	1	0	0.7	10	5	1	0.668204
0.2	2	0.71	5	1	0.66	1	45	0.7	10	5	1	0.670735
0.2	2	0.71	5	1	0.66	1	60	0.7	10	5	1	0.661289
0.2	2	0.71	5	1	0.66	1	30	0.7	10	5	5	0.348693
0.2	2	0.71	5	1	0.66	1	30	0.7	10	5	9	0.0553734
0.2	2	0.71	5	1	0.66	1	30	0.7	10	5	14	−0.274193
0.1	2	0.71	5	1	0.66	1	30	0.7	10	5	1	0.753282
0.3	2	0.71	5	1	0.66	1	30	0.7	10	5	1	0.661833
0.4	2	0.71	5	1	0.66	1	30	0.7	10	5	1	0.668848

Table 3. Sherwood number for different values of parameters

t	R	Pr	M	K	Sc	Sr	α	Du	Gm	Gr	Ec	Sh
0.2	1	0.71	5	1	0.66	1	30	0.7	10	5	1	1.61099
0.2	3	0.71	5	1	0.66	1	30	0.7	10	5	1	1.69869
0.2	4	0.71	5	1	0.66	1	30	0.7	10	5	1	1.71673
0.2	2	4	5	1	0.66	1	30	0.7	10	5	1	1.20522
0.2	2	7	5	1	0.66	1	30	0.7	10	5	1	0.514665
0.2	2	8	5	1	0.66	1	30	0.7	10	5	1	0.0763799
0.2	2	0.71	5	1	1	1	30	0.7	10	5	1	2.15851
0.2	2	0.71	5	1	2.01	1	30	0.7	10	5	1	3.44766
0.2	2	0.71	5	1	3	1	30	0.7	10	5	1	4.64086
0.2	2	0.71	5	1	0.66	4	30	0.7	10	5	1	1.11221
0.2	2	0.71	5	1	0.66	7	30	0.7	10	5	1	0.136135
0.2	2	0.71	5	1	0.66	10	30	0.7	10	5	1	−2.26392
0.2	2	7	5	1	0.66	1	30	0.15	10	5	1	0.654562
0.2	2	7	5	1	0.66	1	30	0.23	10	5	1	0.646871
0.2	2	7	5	1	0.66	1	30	0.5	10	5	1	0.599718
0.2	2	7	5	1	0.66	1	30	0.9	10	5	1	0.25039
0.2	2	0.71	5	1	0.66	1	0	0.7	10	5	1	1.66869
0.2	2	0.71	5	1	0.66	1	45	0.7	10	5	1	1.67248
0.2	2	0.71	5	1	0.66	1	60	0.7	10	5	1	0.68041
0.2	2	0.71	5	1	0.66	1	30	0.7	10	5	5	1.822
0.2	2	0.71	5	1	0.66	1	30	0.7	10	5	9	1.96107
0.2	2	0.71	5	1	0.66	1	30	0.7	10	5	14	2.11779
0.1	2	0.71	5	1	0.66	1	30	0.7	10	5	1	1.8813
0.3	2	0.71	5	1	0.66	1	30	0.7	10	5	1	1.67056
0.4	2	0.71	5	1	0.66	1	30	0.7	10	5	1	1.75187

5. Conclusion

In this work we have analyzed Soret-Dufour and radiation effects on unsteady MHD flow past an inclined porous plate embedded in porous medium in presence of viscous dissipation. From present numerical study the following conclusion can be drawn:

1. Increasing inclination angle, velocity decreases rapidly.
2. Velocity increases slowly, increasing Eckert number.
3. Temperature increases quickly, increasing Eckert number.
4. Concentration decreases afterward increases when Eckert number increases.
5. Velocity increases speedily as Soret number increases.
6. Skin-friction increases when Eckert number and Soret number increase.
7. Skin-friction increases when Dufour number increases.
8. Nusselt number decreases as Eckert number increases.
9. Nusselt number increases when Dufour number, Soret number and Inclination angle increase.
10. Sherwood number decreases as Dufour number and Soret number increase.
11. Sherwood number increases when Eckert number, radiation parameter and Schmidt number increase.

Acknowledgements

We acknowledge the U.G.C. (University Grant Commission) and thank for providing financial support for the research work. We are also thankful to different software companies (Mathematica, MatLab and LaTeX) for developing the techniques that help in the computation and editing.

References

[1] E. M. Sparrow, R. D. Cess, Effect of Magnetic field on free convection heat transfer, Int J Heat Mass Transfer. 3(1961) 267-70.
[2] M. S. Alam, M. M. Rahman, Dufour and Soret effect on MHD free convective Heat and Mass transfer flow past a vertical flat plate embedded in a porous medium, Journal of Noval Architecture and Marine engineering. 2(1)(2005) 55-65.
[3] Z. Dursunkaya, W.M. Worek, Diffusion thermo and thermal Diffusion effects in Transient and Steady natural Convection from vertical surface, International Journal of Heat and Mass Transfer. 35(8)(1992) 2060-2065.
[4] A. Postelnicu, Influence of a Magnetic field on heat and Mass Transfer by natural convection from vertical surface in porous media considering Soret and Dufour effects, International Journal of Heat and Mass Transfer. 47(67)(2004) 1467-1472.
[5] A. Raptis, C. Perdikis, Radiation and free convection flow past a moving plate, Appl. Mech. Eng. 4(4)(1999) 817-821.
[6] V. Rajesh, V. K. Verma, Radiation and mass transfer effects on MHD free convection flow past an exponentially accelerated vertical plate with variable temperature, ARPN Journal of Eng. And App. Sci. 4 (6)(2009) 20-26.
[7] P.V. Satyanarayana, D.Ch. Kesavaiah, S. Venkataramana, Viscous dissipation and thermal radiation effects on Unsteady MHD convection flow past a semi infinite vertical permeable moving porous plate, IJMA. (2011)476-487.
[8] Shivaiah, S. and Anand Rao, J. 2011. Chemical reaction effect on an Unsteady MHD free convective flow past and infinite vertical porous plate with constant suction and heat source. Int. J. of Appl. Math. And Mech. 7(8): 98-118.
[9] M.A. Alabraba, AR. Bestman, A. Ogulu, Laminar convection in binary mixed of Hydro magnetic flow with Radiative Heat Transfer, Astrophysics and Space Science. 195(2)(1992) 431-439.
[10] M.D. Enamul Karim, M.D. Abdus Samad, M.D. Maruf Hasan, Dufour and Soret effect on steady MHD flow in presence of Heat generation and magnetic field past an inclined stretching sheet, Open Journal of Fluid Dynamics. 2(2012) 91-100.
[11] M. Bhavana, D. Kesaraiah Chenna, A. Sudhakarraiah, The Soret effect on free convective unsteady MHD flow over a vertical plate with heat source, Int. J. of Innovative R. in Sci. Eng. And Tech. 2(5)(2013) 1617-1628.

[12] T.G. Cowling, Magnetohydrodynamics, Inter Science Publishers. New York, 1957.
[13] Brice Carnahan, H.A. Luthor, J. O. Wilkes, Applied Numerical Methods, John Wiley and Sons, New York, 1969